

DEVELOPMENT OF A LOW FIELD MRI-BASED APPROACH FOR OBSERVATION OF WATER PENETRATION INTO CLAY: PRELIMINARY RESULTS

By Shivam Gupta

INTRODUCTION

Magnetic resonance imaging (MRI) are considered one of the most efficient and non-invasive methods of observing water content in permeable substances.^{1,3} MRI can visualize and quantify the movement of water in real time.³ In this study, MRI was used to observe the water penetration through clay. Furthermore, MRI can acquire three-dimensional data due to its radio-frequency signals from any orientation.^{2,4} The contrast of the images produced by MRI is a display of the fluid concentration.⁴ As such, any change in the contrast intensity is interpreted as a regional change in the concentration of fluid.^{1,4} This report summarizes the preliminary results from a series of experiments performed with an MRI. The primary goal of the study is to provide a non-destructive method to quantify the permeation of clay using different amounts of water to determine if the low-field MRI approach can be viable option when evaluating the development of storage containers. This investigation is motivated with the intent to develop better and more environmentally friendly containers used to store radioactive waste.

BULK RELAXATION

Bulk Relaxation Measurements including the T_2^* , T_2 and T_1 relaxation time constants for a different Water Content:

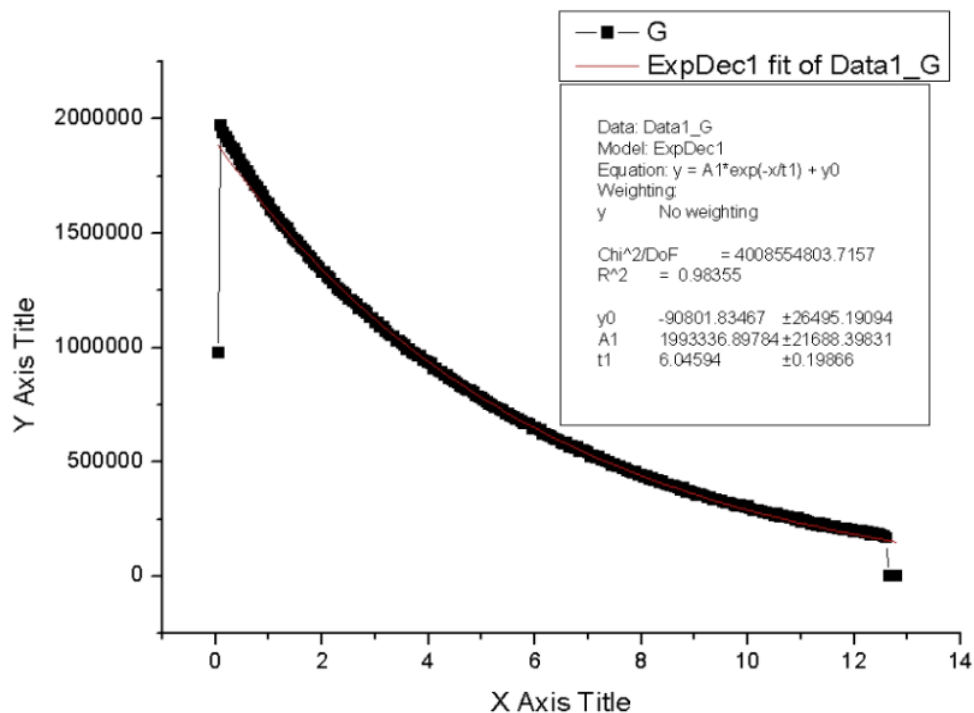


Figure 1. T_2 Decay Curve (dots) and the Best Fit

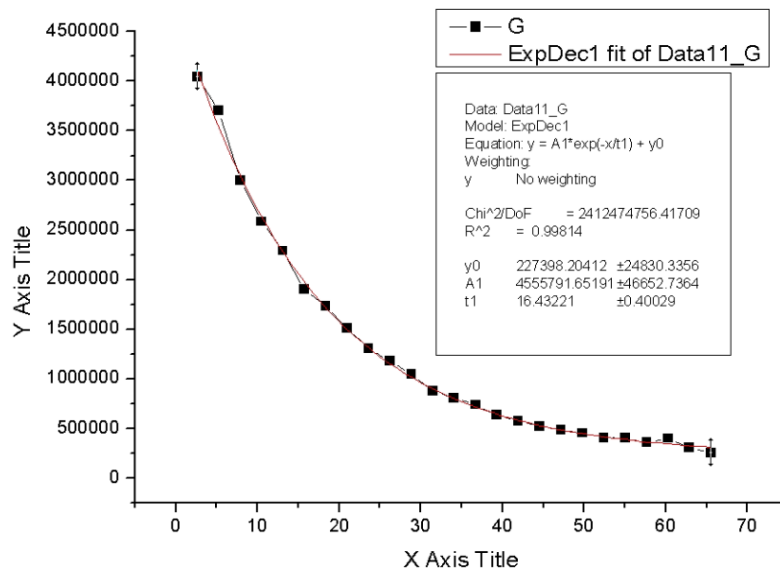


Figure 2. T_2 Decay Curve (dots) and the Best Fit

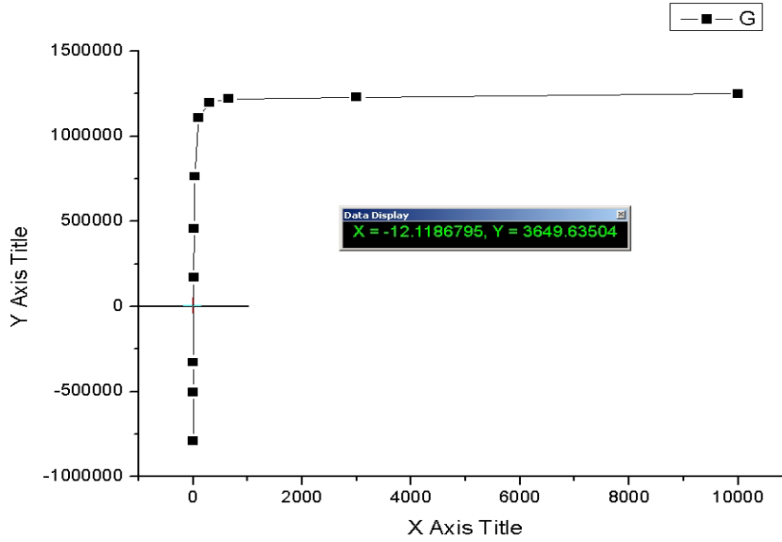


Figure 3. T_1 Recovery Curve (dots) and the Best

Table 1. Relaxation Constants vs Volume of water

| Water Content | $\langle T_2^* \rangle \pm SD$ ms | $\langle T_1 \rangle$ ms | $\langle T_2 \rangle \pm SD$ ms |
|---------------|-----------------------------------|--------------------------|---------------------------------|
| baseline | 3.6 ± 0.08 | 5.5 | 7.3 ± 1.4 |
| +1ml | 4.1 ± 0.10 | 5.5 | 14.5 ± 2.4 |
| +1ml | 4.7 ± 0.12 | 5.5 | 12.7 ± 2.5 |
| +1ml | 5.1 ± 0.13 | 5.5 | N/A |
| +1ml | 5.4 ± 0.15 | 5.5 | 16.4 ± 0.4 |

As the volume of water increases, the values of the relaxation time constants T_2^* and T_2 increases whereas the value of T_1 remains constant.

2D X-CENTRIC PULSE

2D of the Water Content Distribution Imaging with the X-Centric Pulse Sequence

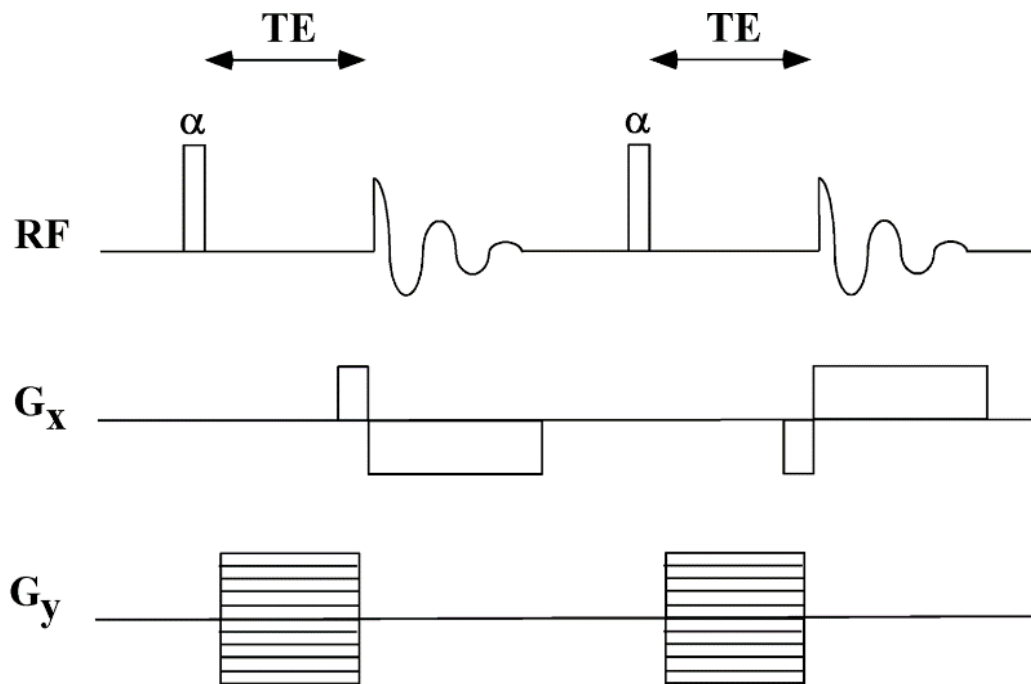


Figure 4. Pulse sequence timing diagram of the X-Centric FGRE acquisition scheme. The X-Centric approach minimizes signal loss due to short T_2^* since the number of k-space points acquired before the center of the k_x line is significantly reduced.

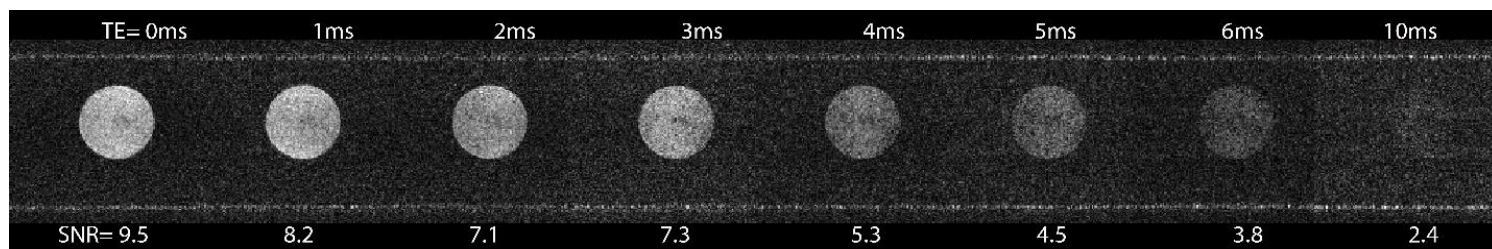


Figure 5. Representative unweighted (TE=0ms) & weighted Images of the Water Content Distribution. The signal degradation of weighted Images reflects the short T_2^* value role.

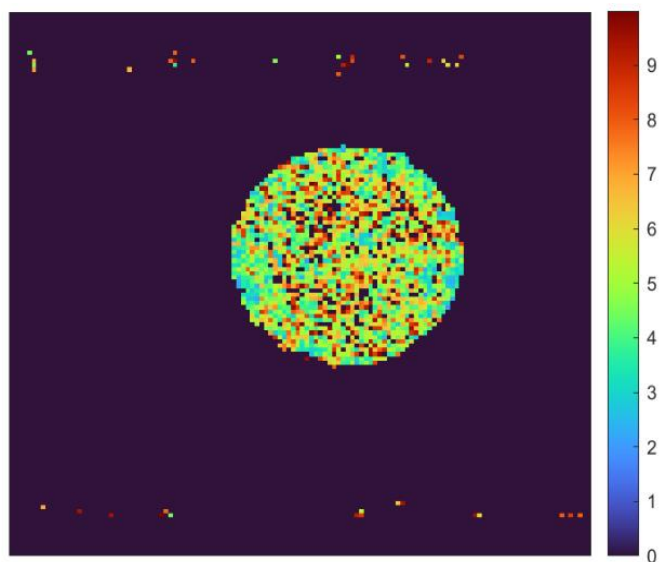


Figure 6. T_2^* -map obtained using the x-centric pulse sequence at nine different echo-times. The map was generated from the images shown in Figure 5.

The map showing a non-uniform T_2^* distribution reflecting a difference in the water content.

FUTURE WORK

3D Imaging of the Water Content Distribution with the X-Centric Pulse Sequence

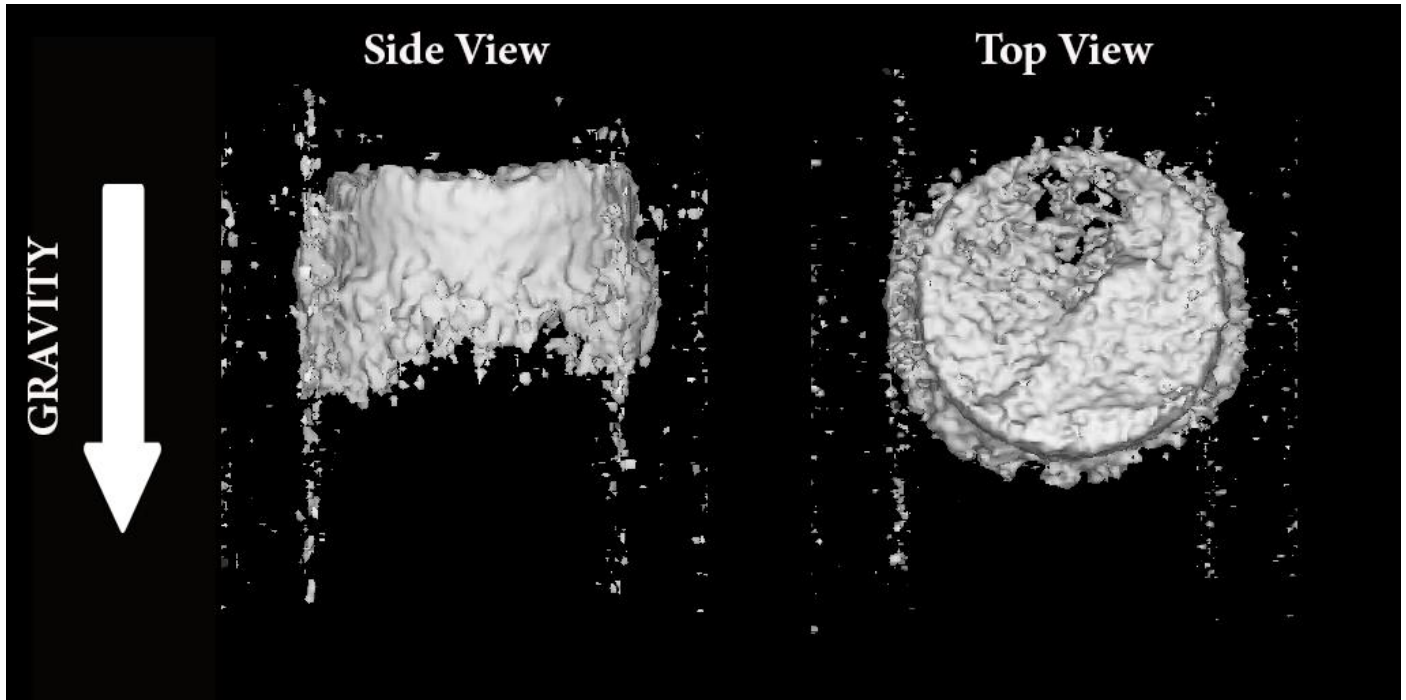


Figure 7. Representative 3D high-resolution image of the water content inside clay obtained at the time-zero. Images was squired with the 3D X-Centric pulse sequence. Image showing the water on top of the clay at the very beginning of the water penetration.

CONCLUSION

Using the low-field MRI we have successfully developed a two-dimensional imaging technique called x-centric for visualizing the water distribution along with T_2^* -mapping. We were also able to acquire three-dimensional images of the water content using 3Dx-centric. Based on the successful imaging results, it is determined that the low-field MRI approach was indeed a successful non-invasive method to quantify the permeation of clay using different amounts of water.

REFERENCES

1. Brown, R. W., Haacke, E. M., Cheng, Y. N., Thompson, M. R., & Venkatesan, R. (2014). *Magnetic resonance imaging: Physical principles and sequence design*. John Wiley & Sons.
2. Dvinskikh, S. V., & Furo, I. (2009). *Magnetic resonance imaging and nuclear magnetic resonance investigations of bentonite systems*. Industrial NMR Centre and Division of Physical Chemistry Department of Chemistry, Royal Institute of Technology.
3. Kishi, T., Yokoyama, Y., Sakai, Y., & Institute of Industrial Science, The University of Tokyo. (2017, July 20). *Non-destructive imaging of water permeation through cementitious materials using MRI*. SCIRP Open Access. <https://www.scirp.org/journal/paperinformation.aspx?paperid=78463>
4. Ouriadov, A. (2020). *The Use of 1H MRI for the Static and Dynamic Visualization and Quantification of the Distribution of Water in Clay: Preliminary Results*. University of Western Ontario/LHRI. https://file:///C:/Users/shiva/Desktop/AOuriadov_Initial_Clay_Report_May11_2020.pdf

APPENDIX

Table 1. T₂ Parameters*

| | | | | | | | |
|---------------------------|-----------|-------------------|------|----------------------|------|----------------------|-----|
| AppendixObs. Freq. | 3.129924 | pw | 186u | Z₂ | 100 | Z_x | 100 |
| Acq. Points | 256 | rd | 300u | Z₃ | 100 | Z_y | 100 |
| Point 1D | 256 | ad | 50u | Z₄ | 120 | | |
| SW +/- | 10000.0Hz | Acq. Time | 12.8 | | | | |
| Filter | 10000.0 | Last Delay | 200m | G_x | 589 | | |
| Dwell Time | 50u | f1 amp | 100 | G_y | 203 | | |
| Acq. Time | 12.8m | f1 attn | 13 | G_z | -150 | | |
| Last Delay | 200m | C13_pw90 | 12u | | | | |
| Obs. Freq. | 3.129924 | pw | 186u | Z₂ | 100 | Z_x | 100 |
| Acq. Points | 256 | rd | 300u | Z₃ | 100 | Z_y | 100 |
| Point 1D | 256 | ad | 50u | Z₄ | 120 | | |
| SW +/- | 10000.0Hz | Acq. Time | 12.8 | | | | |
| Filter | 10000.0 | Last Delay | 200m | G_x | 589 | | |
| Dwell Time | 50u | f1 amp | 100 | G_y | 203 | | |
| Acq. Time | 12.8m | f1 attn | 13 | G_z | -150 | | |
| Last Delay | 200m | C13_pw90 | 12u | | | | |

Table 2. T₁ Parameters

| | | | | | | | |
|--------------------|-----------|-------------------|------|----------------------|------|----------------------|-----|
| Obs. Freq. | 3.129924 | pw | 186u | Z₂ | 100 | Z_x | 100 |
| Acq. Points | 64 | tramp | 500u | Z₃ | 100 | Z_y | 100 |
| Point 1D | 64 | rd | 1m | Z₄ | 120 | | |
| SW +/- | 10000.0Hz | ad | 1u | | | | |
| Filter | 10000.0 | Acq. Time | 3.2m | G_x | 589 | | |
| Dwell Time | 50u | Last Delay | 5s | G_y | 203 | | |
| Acq. Time | 3.2m | F1 Ampl | 100 | G_z | -150 | | |
| Last Delay | 5s | F1 Attn | 13 | | | | |

Table 3. T₂ Parameters

| | | | | | | | |
|--------------------|-----------|-------------------|----------|----------------------|------|----------------------|-----|
| Obs. Freq. | 3.129924 | pw | 168u | Z₂ | 100 | Z_x | 100 |
| Acq. Points | 40 | ad | 50u | Z₃ | 100 | Z_y | 100 |
| Point 1D | 1000 | Tacq/2 | 1.31072m | Z₄ | 120 | | |
| SW +/- | 10000.0Hz | pw2 | 350u | | | | |
| Filter | 10000.0 | Acq. Time | 2m | G_x | 600 | | |
| Dwell Time | 50u | Last Delay | 1s | G_y | 200 | | |
| Acq. Time | 2m | f1 amp | 100 | G_z | -200 | | |
| Last Delay | 1s | f1 attn | 13 | | | | |